High-pressure EXAFS measurements of crystalline Ge using nanocrystalline diamond anvils

M. Baldini,[1,2] W. Yang,[2] G. Aquilanti,[3] L. Zhang,[4] Y. Ding,[2] S. Pascarelli,[5] and W. L. Mao[1,6,7]

[1]*Geological and Environmental Science, Stanford University, 94305 California, USA*

[2]*HPSynC, Geophysical Laboratory, Carnegie Institution of Washington, 9700 South Cass Avenue, Argonne, Illinois 60439, USA*

[3]*Sincrotrone Trieste, Area Science Park s.s.14 Km. 163.5, I-34149 Basovizza Trieste, Italy*

[4]*Geophysical Laboratory, Carnegie Institution of Washington, Washington, DC 20015, USA*

[5]*European Synchrotron Radiation Facility, BP 220, F-38043 Grenoble, France*

[6]*Stanford Institute for Materials and Energy Science, SLAC National Accelerator Laboratory, 2575 Sand Hill Road, Menlo Park 94025 California, USA*

[7]*Photon Science, SLAC National Accelerator Laboratory, Menlo Park, California 94025, USA*

(Received 8 April 2011; published 27 July 2011)

High-pressure extended x-ray absorption fine structure (EXAFS) measurements on crystalline Ge demonstrate that the use of nanocrystalline diamond anvils can solve the glitch problem from single crystal diamond anvils and improve the quality of the data. Our results indicate that using nanocrystalline diamond anvils for high-pressure EXAFS research can provide a large enough energy range for structural study up to four coordination shell distances. In particular, we obtained the pressure evolution of mean square relative displacement for the first neighbor shells of crystalline Ge and observed different correlation effects for different coordination shells. The use of nanocrystalline diamond anvils will provide a breakthrough for high-pressure EXAFS study, especially for amorphous compounds in which only limited structural information can be obtained by diffraction techniques.

DOI: 10.1103/PhysRevB.84.014111 PACS number(s): 61.05.cj, 07.35.+k

I. INTRODUCTION

Structures of liquid, amorphous and crystalline materials are dramatically changed by the application of pressure. Synchrotron x-ray absorption fine structure spectroscopy (EXAFS) represents a powerful tool for probing element-specific local structural changes under compression.[1] However, there are a number of challenges associated with conducting EXAFS studies in a high-pressure diamond-anvil cell (DAC). Typically 2.5-mm-thick single-crystal diamonds are opaque to the low-energy absorption edges. A major difficulty also comes from the strong Bragg reflections from the single crystal diamond anvils, which produce distortions on the EXAFS spectra and reduce the data quality.[2] Consequently, the full potential of the EXAFS technique has not been realized for the full pressure-temperature capability of a DAC (300 GPa-5000 K).

The energy-dispersive x-ray absorption spectroscopy technique has proven to be effective for addressing some of the challenges represented by diamond glitches.[3,5] The strongly focusing crystal and the absence of movement provide the small and stable focal spot necessary for high-pressure measurements. The entire spectral range is observed simultaneously, which makes finding the optimum cell orientation with the widest glitch-free energy range much easier and efficient. The data acquisition process is much faster than conventional scanning EXAFS method but the glitch-free energy range is still limited.[4] The presence of diamond Bragg peaks limits the k range and adversely affects the quality of the data. For example, the effect of disorder on the amplitude of the EXAFS signal is generally accounted for by an EXAFS Debye-Waller factor $\exp -2\sigma^2 k^2$, where σ^2 is the mean-square relative displacement of absorber and back-scatterer atoms. A precise evaluation of the σ^2 parameters requires collecting data in an extended k range since σ^2 determines the rate of decay of the EXAFS oscillations at high k through the exponential term. Whereas there is no intrinsic limitation to the measurable k range for ambient pressure EXAFS measurements, this remains a major problem for high pressure EXAFS due to the Bragg diffraction from the diamond anvils. Moreover, limitations in k range also means that a reduced number of independent parameters is available for the quantitative data analysis, making difficult to consider high coordination shells and multiple-scattering effects.

In this work, we present high-pressure EXAFS measurements performed on crystalline Ge up to 17 GPa, employing for the first time a DAC with nanocrystalline diamond (ND) anvils. Polycrystalline diamond, which consists of nano-sized randomly oriented diamond grains, can be synthesized by direct conversion of graphite under static high pressure and high temperature.[6] ND anvils have been used to generate pressures above 200 GPa,[7] comparable to the pressure range for single-crystal diamond anvils.

Crystalline Ge was chosen as a reference system since the structural transition observed at approximately 11 GPa has been widely investigated.[8–10] We demonstrate that the use of ND addresses the problem caused by diamond glitches. The quality of the high-pressure data is comparable to data obtained from an amorphous Ge foil (a standard calibrant) at ambient conditions. The pressure evolution of bond lengths R_{Ge-Ge} and mean-square relative displacements σ^2 was obtained up to high-coordination shells, providing original information on correlation effects for each coordination shell, information which is unaccessible to diffraction techniques.[11–13] To further underscore the advantages of using ND anvils, the results were compared with EXAFS results obtained using single-crystal diamond anvils and with those extracted from x-ray diffraction (XRD) data. Our results prove that ND are effective in removing the diamond glitches and opens up new opportunities for high-pressure EXAFS measurements.

II. EXPERIMENTAL

ND cylinders were synthesized from graphite in a multianvil apparatus at 20 GPa and 2500 K and then shaped and polished to be used as anvils. Single-crystal perforated anvils of 1.5-mm thickness and with a 300-μm-diameter hole were employed as diamond-backing plates. ND anvils with 250-μm-diameter culets were placed on top of perforated diamonds. The thickness of the ND anvils was 900 μm. Perforated diamonds reduce the diamond absorption and ND anvils avoid the single-crystal glitches. Ge powder was loaded without any pressure medium into a 100-μm -diameter hole drilled in a preindented tungsten gasket. The pressure was measured *in situ* with the ruby fluorescence technique.[14] The measurements were performed up to 17 GPa with ND anvils and up to 60 GPa with single-crystal diamond anvils. X-ray absorption spectra were collected at the ID24 dispersive EXAFS beam line of European Synchrotron Radiation Facility (ESRF).[3] The energy dispersive spectrometer employed a bent crystal to focus and disperse a polychromatic x-ray beam onto the sample. The beam, passing through the sample, diverges toward a position sensitive detector, in which the pixel position is correlated to the x-ray energy. The x-ray beam with an energy window around the Ge K edge, was focused both in the horizontal and in the vertical planes to a 10 × 10-μm spot. Each spectrum was collected 100 times and averaged after background subtraction and normalization.

III. EXPERIMENTAL RESULTS AND QUANTITATIVE DATA ANALYSIS

In Fig. 1, the EXAFS signals of Ge collected at 8.7 GPa using single-crystal diamonds and ND anvils are compared with the signal from standard amorphous Ge foil collected at ambient conditions to energy-calibrate the data. The EXAFS function obtained with ND anvils is comparable to the one from the a-Ge foil, demonstrating that employment of ND anvils

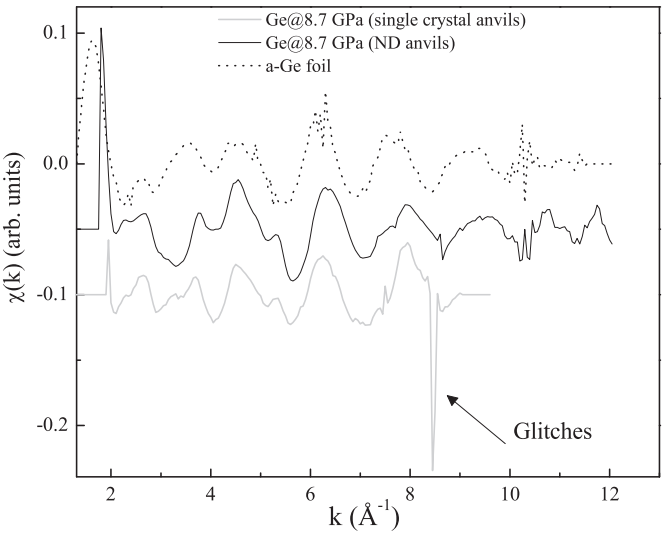

FIG. 1. EXAFS signal of Ge obtained with ND anvils (black line) and single-crystal anvils (grey line). EXAFS function of standard amorphous Ge foil obtained without DAC (dotted line). An offset was added to the EXAFS signals.

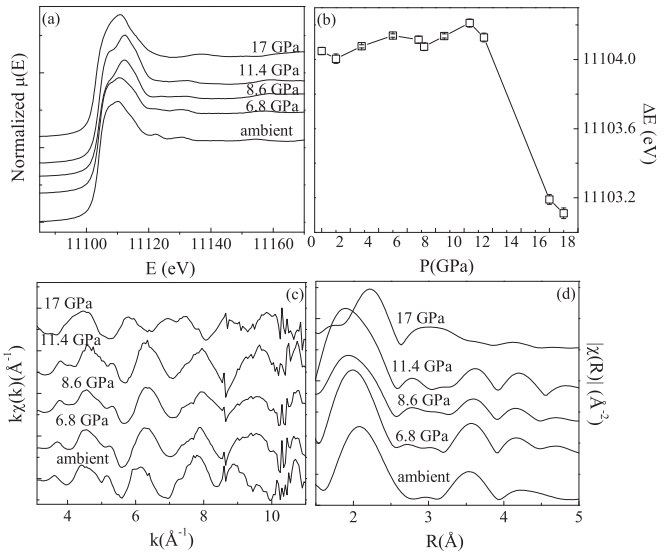

FIG. 2. Normalized XANES absorption spectra at selected pressures (a). Evolution of the edge position with pressure (b). Extracted EXAFS signals kχ(k) Å^{-1} at selected pressure (c). Moduli of the Fourier transform of the experimental EXAFS spectra (d).

provides a clear advantage in data quality at high pressure. The features observed around 10 Å^{-1}, which are also seen in the spectrum from Ge foil, are due to the beamline optics and do not significantly impact the data. The Bragg reflections from single-crystal diamonds start to be observed above 8 Å^{-1} in the gray spectrum, after optimization of the cell position, and limit the available k range to 7 Å^{-1}.

The x-ray absorption near edge spectroscopy region is shown in Fig. 2(a) for selected pressures. The spectra were normalized to the jump at the absorption edge. Changes in near edge region are observed above 11 GPa because of a structural transition from a cubic diamond phase to a tetragonal β-Sn phase.[8–10] The large energy decrease (∼1 eV) around 11 GPa in the pressure evolution of the absorption edge in Fig. 2(b), is consistent with the semiconductor to metal transition occurring simultaneously with the structural transformation.[8–10] The EXAFS signal $\chi(k)$ was obtained by subtracting the embedded-atom absorption background from the measured absorption coefficient and normalizing by the edge step. The k-weighted $\chi(k)$ EXAFS signal and the moduli of the Fourier transform at selected pressures are shown in Figs. 2(c) and 2(d). At ambient pressure, the main contribution to the EXAFS signal is the single scattering between the Ge atom and the nearest neighbors [peak around 2.0 Å in Fig. 2(d)]. The two peaks around 3.5 Å and 4.5 Å result from contributions from higher shells. The changes of the EXAFS signal observed at 17 GPa in Figs. 2(c) and 2(d) are the spectral signature of the structural transition from the cubic diamond phase to the tetragonal β-Sn phase.

Quantitative analysis of the EXAFS signals was carried out with the ARTEMIS package.[15] Back-scattering amplitudes and phases were calculated with the FEFF6 code using a fourfold cubic diamond structural model for the data collected below 11 GPa and a sixfold tetragonal β-Sn structure for the

data collected above the transition. The amplitude reduction factor S_0^2 and the energy shift E_0 were fixed to values obtained from the analysis of the standard a-Ge foil collected before each EXAFS measurement. S_0^2 was found to be equal to 1.1 ± 0.1, while E_0 to 3 eV and was slightly varied (± 2 eV) depending on the k, R ranges and model used. In Table I, we list k range, R range, and the model (fitting parameters) used in the analysis of the data collected with the ND anvils and the single crystal anvils, for both the diamond and the β-Sn phase.

The k range for the Ge EXAFS data collected with single crystal diamonds is limited to 3–7 $Å^{-1}$ by the presence of Bragg reflections [Fig. 3(b)]. Therefore, only the first shell Ge-Ge path was used to model the data in the diamond phase with the bond distance R_{Ge-Ge_1} and the Debye Waller factor σ_1^2 as free parameters (Table I). In the β-Sn phase, the sixfold coordinated Ge atom displays two nonequivalent first neighbor Ge-Ge distances: $R_{Ge-Ge_1} = 2.56$ Å and $R_{Ge-Ge_2} = 2.72$ Å. Since these values are so close to each other, a strong correlation between the first neighbor bond distances R_{Ge-Ge_1} and R_{Ge-Ge_2} and relative Debye Waller factors is observed. The pressure dependence of the first neighbor Ge-Ge distances was thus treated forcing a uniform compression described by the following math expression $R_{Ge-Ge_n}(P) = R_{Ge-Ge_n}(P = 0)[1 + a]\,(n = 1,2)$, with $\sigma_1^2 = \sigma_2^2, a$, and σ_1^2 as free parameters (Table I). A best fit result is shown in Fig. 3(b). The pressure evolution of the Ge-Ge bond lengths obtained for the EXAFS data collected with single-crystal diamonds is reported in Fig. 3(c). Due to the limited k range, mean-square relative displacements do not display reliable values (due to very large error bars) and are not reported.

TABLE I. k range and R range considered for both sets of data. Parameters used for fitting the data in the diamond and the β-Sn phase.

Diamond phase		
Parameters	ND anvils	Single crystal anvils
k range ($Å^{-1}$)	3.1–10.5	3–7
R range (Å)	1.5–4.8	1.8–3.0
R_{Ge-Ge} (Å)	R_{Ge-Ge_1} R_{Ge-Ge_2} R_{Ge-Ge_3}	R_{Ge-Ge_1}
σ^2 ($Å^2$)	σ_1^2 σ_2^2 σ_3^2	σ_1^2
β Sn phase		
Parameters	ND anvils	Single crystal anvils
k range ($Å^{-1}$)	3.1–10.5	3–7
R range (Å)	1.7–3.9	1.5–3.4
R_{Ge-Ge} (Å)	a R_{Ge-Ge_3} R_{Ge-Ge_4}	a
σ^2 ($Å^2$)	$\sigma_1^2 = \sigma_2^2$ σ_3^2 σ_4^2	$\sigma_1^2 = \sigma_2^2$

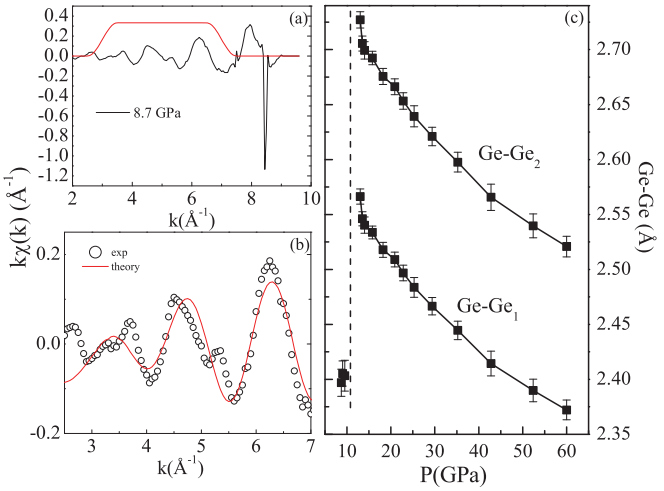

FIG. 3. (Color online) EXAFS signal $\chi(k)$ and the Hanning window used for the Fourier transformation. Results of the quantitative analysis performed on Ge EXAFS data collected using single-crystal diamond anvils. Best fit result at 8.7 GPa (b). Pressure dependence of the Ge-Ge bond lengths up to 60 GPa (c).

In contrast, contributions from higher shells were considered for the data collected with ND anvils since a wider k range was available. In the diamond phase, three Ge-Ge paths were used to model the data. The quantitative fit was performed considering each one of the three Ge-Ge bond distances and the relative σ^2 as free parameters (Table I). For the β-Sn phase, contributions up to the fourth shell were taken into account. A uniform compression was considered for the first neighbor bond distances so the free parameters used for the quantitative analysis were: a for the first two bond lengths, R_{Ge-Ge_3}, R_{Ge-Ge_4}, σ_1^2, σ_3^2, and σ_4^2 (Table I). A best fit result

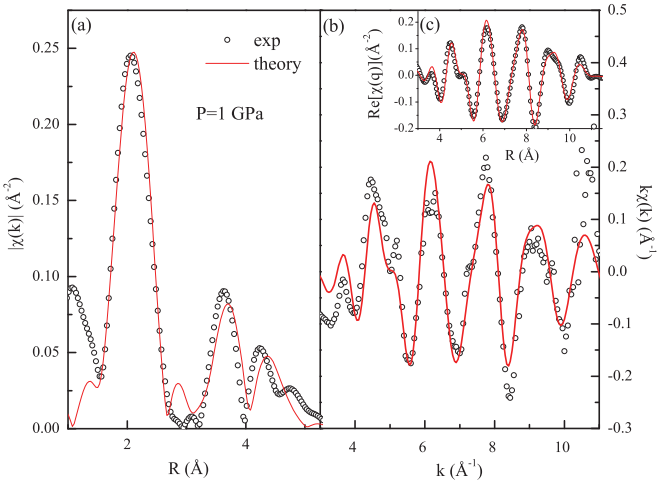

FIG. 4. (Color online) Comparison between the experimental EXAFS spectrum collected with ND anvils at 1 GPa (dots) and the best-fit calculation (solid curve) using three Ge-Ge paths. Comparison is reported for the moduli of the Fourier transform (a), the extracted kχ(k)Å^{-1} signal (b), and for the real part of the back-transformed signal (c).

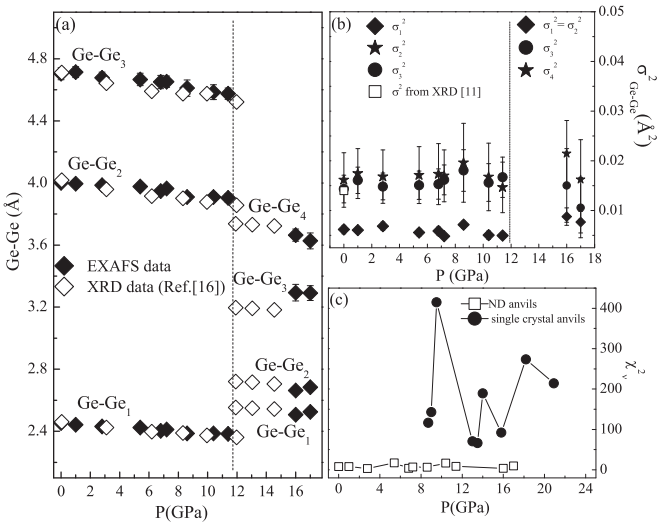

FIG. 5. Results of the quantitative analysis performed on Ge EXAFS data collected using ND anvils. Pressure dependence of the Ge-Ge bond distances (a). Pressure dependence of the Debye Waller factor (b). Pressure dependence of χ^2_ν obtained analyzing the data collected with ND and single-crystal diamond anvils (c).

is reported in Fig. 4 and compared with the experimental spectrum collected with ND anvils.

The Ge-Ge bond lengths and relative σ^2 obtained using ND anvils are displayed in Figs. 5(a) and 5(b). It is evident that the use of ND anvils assures a more detailed quantitative analysis. Pressure dependence of the bond distances was obtained up to the third shell for the diamond phase and up to the fourth shell for the β-Sn phase [Fig. 5(a)]. The first neighbor Ge-Ge bond distances are found to increase above the transition because of the change from fourfold to sixfold coordination. On the other hand, higher shell bond distances are found to decrease above the transition, consistently with the high-pressure β-Sn structure being more tightly packed than the diamond phase. The results on interatomic distances are in good agreement with bond lengths extracted from XRD data,[16] as expected for a monoatomic single-crystalline phase.

In the case of monoatomic crystals, local structural parameters such as number of nearest neighbors and interatomic distances can all be derived from crystallographic parameters obtained by x-ray diffraction technique. However, EXAFS is sensitive to the correlation of atomic motion[11–13] and, unlike diffraction methods that monitor uncorrelated mean square displacement, the σ^2 parameter contains also the contribution from the displacement correlation function. Indeed, the EXAFS parameter σ^2 corresponds to the mean-square relative displacement along the different bond directions between the absorber and the scatterer atoms.[13] The pressure evolution of σ^2 for the nearest neighbor shells are reported in Fig. 5(b). In the diamond phase, ambient pressure values $\sigma^2_1 = (6 \pm 1)10^{-3}$ Å^2 and $\sigma^2_2 \sim \sigma^2_3 = (15 \pm 5)10^{-3}$ Å^2 are in good agreement with previous EXAFS data.[11,17] These reflect a first shell correlation stronger than expected, whereas higher coordination shell values approach those measured by x-ray diffraction [empty square in Fig. 5(b)]. Values are found not be affected by compression within the error bars, up to the structural phase transition. In the β-Sn phase at 16 GPa, $\sigma^2_1 = (8 \pm 1)10^{-3}$ Å^2, $\sigma^2_2 = (15 \pm 5)10^{-3}$ Å^2, and $\sigma^2_3 = (22 \pm 5)10^{-3}$ Å^2. First-shell values are larger due to larger interatomic distances and σ^2 values are found to increase for higher coordination shells, reflecting progressively lower correlation in atomic motion with distance. This finding is consistent with more the"metallic" character of the bonds in the β-Sn phase with respect to the stronger "covalent" nature of bonding in the diamond phase. In Fig. 5(c), we report the pressure evolution of the reduced χ^2_ν, which provides a further demonstration that the quality of the fit is better for the data collected with ND anvils.

Alternative methods to attain good quality EXAFS data at high pressure have been presented over the years. For example, glitches can be moved out of the region of interest by DAC rotation. Each rotation moves the glitches to new positions. Collecting a new set of data for each DAC position, the glitches can be manually removed and the spectra added together afterwards.[18] A similar approach for acquiring high-quality EXAFS data using DAC was recently reported.[19] In this study, the diamond glitches are eliminated using an iterative algorithm based on repeated measurements over a small angular range of DAC orientation. In both cases, the collected data need to be iteratively processed in order to eliminate the diamond glitches.

Another way to address this problem is to use large volume Paris-Edinburgh press[20] or multi-anvil presses.[21] Boron carbide (B_4C)[22] or sapphire anvils[23] also allow collection of EXAFS data free from diffraction peaks. For both of these methods—the first one based on the DAC rotation, the second one based on the use of devices different from DAC present disadvantages—either the data need to be further processed or the pressure range accessible is strongly limited. The use of ND anvils addresses both issues and provides high-quality EXAFS spectra.

In conclusion, we performed the first high-pressure EXAFS experiment using a DAC with ND anvils. We demonstrate that ND anvils are effective in avoiding the Bragg reflections from the single-crystal diamonds. The quality of the collected data appears comparable to those obtained outside the DAC and represents an evident increase of the extent of k range available. Previous high-pressure EXAFS experiments performed on this system limited the results to the first shell.[16,17] Results obtained with the quantitative analysis provided information up to the third shell for the diamond phase and up to the fourth shell for the β-Sn phase, demonstrating that the employment of ND anvils offers evident advantages for coupling EXAFS and DAC techniques. In the case of a monoatomic system such as crystalline Ge, the EXAFS derived σ^2 values provide complimentary information on correlation effects for each coordination shell. This experiment demonstrates that it is possible to perform a more detailed analysis with ND anvils and to recover more accurate information about the local structure. This is crucial for amorphous compounds, which cannot be investigated with XRD techniques. Our results expand the opportunities for using EXAFS to characterize material at high pressure.

ACKNOWLEDGMENTS

This work is supported by the Department of Energy, Office of Basic Sciences, Division of Material Science and Engineering under Contract No. DE-AC02-76SF00515. W. Mao is also supported through the Geophysics program at NSF (Grant No. EAR-0738873). HPSynC is supported as part of EFree, an Energy Frontier Research Center funded by DOE-BES under Award No. DE-SC0001057. L. Zhang is supported by the NSF Geophysics EAR-0911492.

[1] J.-P. Itie, F. Baudelet, E. Dartyge, A. Fontaine, H. Tolentino, A. San Miguel, High Pres. Res. **8**, 697 (1992).
[2] A. V. Sapelkin and S. C. Bayliss, High Press. Res. **21**, 315 (2001).
[3] S. Pascarelli, O. Mathon, M. Munoz, T. Mairs, and J. Susini, J. Synchrotron Radiat. **13**, 351 (2006).
[4] S. Pascarelli, O. Mathon, and G. Aquilanti, J. Alloys Compd. **362**, 33 (2004).
[5] M. Baldini, G. Aquilanti, H-k. Mao, W. Yang, G. Shen, S. Pascarelli, and W. L. Mao, Phys. Rev. B **81**, 024201 (2010).
[6] T. Irifune, A. Kurio, S. Sakamoto, T. Inoue, and H. Sumiya, Nature (London) **421**, 599 (2003).
[7] Y. Nakamoto, H. Sumiya, T. Matsuoka, K. Shimizu, T. Irifune, and Y. Ohishi, Jpn. J. Appl. Phys. **46**, L640 (2007).
[8] H. Olijnyk, S. K. Sikka, and W. B. Holzapfel, Phys. Lett. A **103**, 37 (1984).
[9] C. S. Menoni, J. Z. Hu, and I. L. Spain, Phys. Rev. B **34**, 362 (1986).
[10] A. Di Cicco, A.-C. Frasini, M. Minicucci, E. Principi, J.-P. Itie, and P. Munsch, Phys. Status Solidi B **240**, 19 (2003).
[11] G. Dalba and P. Fornasini, J. Synchrotron Radiat. **4**, 243 (1997).
[12] G. Beni and P. M. Platzman, Phys. Rev. B **14**, 1514 (1976).
[13] A. Yoshiaka, K. Koto, H. Maeda, and T. Ishii, Jpn. J. Appl. Phys. **36**, 781 (1997).
[14] H.-K. Mao, J. Xu, and P. M. Bell, J. Geophys. Res. **91**, 4673 (1986).
[15] J. J. Rehr and R. C. Albers, Rev. Mod. Phys. **72**, 621 (2000); B. Ravel and M. Newville, J. Synchrotron Radiat. **12**, 537 (2005).
[16] A. Di Cicco, E. Principi, M. Minicucci, S. De Panfilis, A. Filipponi, F. Decremps, F. Datchi, J.-P. Itié, P. Munsch, and A. Polian, High Press. Res. **24**, 93 (2004).
[17] A. Yoshiasa, T. Nagai, O. Ohtaka, O. Kamishimab, and O. Shimomurac, J. Synchrotron Radiat. **6**, 43 (1999).
[18] Andrei V. Sapelkin, Sue C. Bayliss, Dean Russell, Simon M. Clark, and Andy J. Dent, J. Synchrotron Radiat. **7**, 257 (2000).
[19] X. Hong, M. Newville, V. B. Prakapenka, M. L. Rivers, and S. R. Sutton, Rev. Sci. Instrum. **80**, 073908 (2009).
[20] Y. Katayama, M. Mezouar, J. P. Itie, J. M. Besson, G. Syfosse, P. Le Fevre, and A. Di Cicco, J. Phys. IV (France) **7**, C2-1011 (1997).
[21] Y. Katayama, K. Tsuji, O. Shimomura, and H. Oyanagi, J. Non-Cryst. Solids **205-207**, 199 (1996).
[22] Sarah H. Tolbert and A. P. Alivisatos, Annu. Rev. Phys. Chem. **46**, 595 (1995).
[23] K. Tamura, S. Hosokawa, M. Inui, M. Yao, H. Endo, and H. Hoshino, J. Non-Cryst. Solids **150**, 351 (1992).